Smart Energy 14 (2024) 100143

Contents lists available at ScienceDirect

Smart Energy

journal homepage: www.journals.elsevier.com/smart-energy

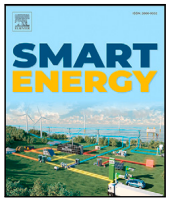

Coordinating multiple Power-To-Gas plants for optimal management of e-fuel seasonal storage

Emanuela Marzi [a,*], Mirko Morini [a,b], Costanza Saletti [a], Agostino Gambarotta [a,b]

[a] Department of Engineering and Architecture, University of Parma, Parco Area delle Scienze 181/A, Parma, 43124, Italy
[b] Center for Energy and Environment (CIDEA), University of Parma, Parco Area delle Scienze 42, Parma, 43124, Italy

ARTICLE INFO

Keywords:
Multi-energy systems
Power-to-gas
Long-term storage
Model predictive control
Hierarchical control

ABSTRACT

Seasonal storage is a key feature of future decarbonized energy systems with a high share of renewable energy integration. Power-to-Gas technologies represent a promising solution to enable such storage. They allow the conversion of surplus renewable electricity into e-fuels and their storage in the long-term. Their utilization enables the integration of the electrical, fuel and heating sectors, by converting electricity into fuels and recovering the waste heat from the process. Nevertheless, to design the most profitable management strategy for such systems, advanced control tools are required. This study introduces a novel control architecture for multiple multi-energy systems that share an e-fuel seasonal storage. Each energy system has its own short-term control logic, based on Model-Predictive Control (MPC), which manages day-ahead energy exchanges, while a long-term MPC controller considers yearly dynamics and the system as a whole. This gives additional constraints to the short-term controllers, which ensure the fulfillment of yearly goals. A multi-temporal and multi-spatial hierarchical control architecture is proposed, which enables optimal seasonal storage management, and its operation is verified in a Model-in-the-Loop configuration. The controller efficiently uses seasonal storage to balance seasonal mismatch between production and demand, resulting in higher utilization of renewable energy, lower emissions and costs.

1. Introduction

In response to the need to reduce carbon dioxide emissions in the energy sector, significant efforts are currently underway to promote the exploitation of distributed and non-programmable renewable energy sources (RES). This transformation is reshaping the structure of existing energy systems, which need to become more flexible. Indeed, the mismatch between energy generation and consumption poses challenges, introducing complexity that requires the integration of innovative technologies and technical solutions. Consequently, this is reshaping the traditional approach to energy system management and emphasizes the importance of embracing the Multi-Energy System (MES) concept [1], which involves considering energy systems as a whole and optimizing overall energy exchanges, encompassing the integration of different sectors.

Within this framework, Power-to-Gas (PtG) technologies have gained considerable significance by facilitating the integration of various sectors through the production of synthetic fuels derived from renewable electricity, also known as e-fuels or electrofuels [2]. Notably, the PtG process encompasses two main stages: the electrolysis process, by which electricity is converted into hydrogen using an electrolyzer, and the methanation process, by which synthetic methane is generated by combining hydrogen and carbon dioxide into a catalytic reactor. In this framework, many technologies exist, as well as real-world projects that aim to study the benefits of generating such fuels from renewable electricity [3].

These fuels can serve not only as conventional energy sources but also be converted back into electricity when needed, being an efficient energy storage solution that reduces the wasteful curtailment of renewable energy resources. The integration of PtG solutions into integrated energy systems further enhances this potential, enabling bidirectional interconnections between electrical and gas networks by using excess renewable electricity to generate sustainable fuels [4].

In recent years, numerous studies in the field of PtG have been conducted, along with pilot and demonstration projects [5,6]. At the same time, there is an increasing focus on enhancing the thermal management of these technologies to unlock possibilities for combined heat and power generation, while improving infrastructure interconnectivity, increasing efficiency and lowering fuel cost. These initiatives not only facilitate the long-term chemical storage of excess renewable energy, but also alleviate congestion in both gas and electricity networks [7].

* Corresponding author.
E-mail address: emanuela.marzi@unipr.it (E. Marzi).

https://doi.org/10.1016/j.segy.2024.100143
Received 31 January 2024; Received in revised form 17 April 2024; Accepted 18 April 2024
Available online 25 April 2024

Even though PtG plants currently face economic efficiency challenges, ongoing developments in these technologies and their implementation into integrated energy systems are expected to alter this scenario. Indeed, as global awareness of sustainable energy transformation rises, PtG technologies will gain substantial advantages from evolving energy policies. Moreover, the prospect of multiple coordinated energy systems, coupled with strategically implemented PtG plants and shared seasonal storage units, holds promise in offering alternative solutions for future energy systems [8].

Nevertheless, to effectively manage the interaction among gas, electricity, and district heating networks for achieving energy systems decarbonization, it is not enough to install sufficient capacity. Instead, it is crucial to intelligently coordinate and operate the various plants. Indeed, the integration of different components into the system and their operating strategies significantly impact their performance. Traditional controllers, relying on fixed time schedules or priority rules, are inadequate in addressing these challenges as they lack tailored solutions adapted to real-time conditions. Therefore, the implementation of smart control tools becomes imperative. For this reason, there is currently substantial interest among researchers and industries in exploring and implementing novel control strategies and optimization tools in practical systems, which is essential for facilitating the integration of emerging technologies and facilitating sector integration.

According to Alabi et al. [9], the main innovative energy management techniques capable of considering the dynamic behavior of energy systems and effectively controlling them are Model Predictive Control (MPC) and Deep Reinforcement Learning (DRL). MPC is an advanced control technique which allows the optimal control of complex systems by employing an optimization algorithm that incorporates a simplified model of the system to be controlled [10,11]. On the other hand, DRL is a machine learning-based technique, that has recently gained prominence in the context of managing MES [12]. It employs a reinforcement learning agent to interpret the system, dynamically learning through a deep learning approach, and adjusting its actions based on feedback from the system. Nevertheless, despite the advantages of DRL, its literature is relatively underdeveloped compared to MPC and presents certain drawbacks. These include the substantial offline computational cost required for training and challenges in effectively managing constraints [13,14]. Instead, the incorporation of a detailed model within an MPC algorithm facilitates a more straightforward evaluation of the control action. Additionally, for complex systems, model-based controllers like MPC can be easily tailored to the specific case study, and with the use of a suitable optimization algorithm, online computational efficiency can be achieved. For these reasons, MPC was selected in this work.

For the purpose of this study, a control strategy based on MPC was developed, which is capable of addressing multiple space and time scales, and optimally managing the operation of a seasonal e-fuel storage system. As far as the authors know, numerous studies in the existing literature have underscored the potential energy savings that can be achieved through the implementation of predictive controllers, which enable optimal system management. In addition, MPC has demonstrated its effectiveness as a control method for optimizing the operation of PtG technologies, especially when integrated into complex MES [15]. Nevertheless, the challenge that this work faces is the ability of the control action to incorporate information concerning long-term changes in external factors that influence the behavior of the system and to consider the interaction of multiple energy systems sharing seasonal storage. This becomes crucial when a seasonal storage component is included, and it is evident that effectively optimizing the seasonal storage capabilities of the system is a complex task [16]. Nonetheless, the utilization of PtG technologies for seasonal storage shows promise and warrants further investigation.

1.1. Literature review

In the literature some studies already exist that apply MPC strategies to seasonal energy storage integrated into MES. For instance, Thaler et al. [17] develop an MPC in which the seasonal dynamics related to hydrogen storage are incorporated through the inclusion of a hydrogen cost term as a revenue in the objective function. When there is excess renewable energy, the objective function incentivizes hydrogen production and its storage in the long term. Indeed, when implementing a PtG system for seasonal storage, it becomes crucial to account for the annual dynamics governing its management. Nevertheless, optimizing the entire year with real-time control time-steps poses a computational challenge. To overcome this issue, Weber et al. [18] developed a control architecture based on MPC featuring two controllers with distinct time scales for managing seasonal thermochemical storage in buildings. This involves a higher-level annual scheduling objective-based controller and a lower-level tracking-MPC that flexibly follows the trajectory set by the high-level controller. Similarly, in [19], the authors introduced a novel control strategy for the optimal management of microgrids with a high penetration of RES and various energy storage systems. A supervisory MPC generates optimal scheduling using a statistical approach to address uncertainties in weather and load forecasting. Specifically, long-term optimization of microgrid components is achieved through optimal generation scheduling, while real-time system management relies on a short-term MPC module utilizing the results obtained with the optimal generation scheduling. In this way, both short- and long-term optimal planning schedules are realized through the application of an MPC.

A similar work was done by Zhang et al. [20]. The authors presented a strategy for multiple time-scale optimization, incorporating both multi-day forecast information and intra-day MPC. The intra-day MPC is executed by considering multi-day forecasts, employing hierarchical rolling optimization to adjust day-ahead scheduling, and utilizing MPC to address uncertainties in renewable energy sources and loads. Darivianakis et al. [16] introduced a data-driven stochastic predictive control scheme tailored for the efficient management of energy hubs equipped with seasonal storage capabilities. This scheme captures the long-term operation of the system through a value function, utilizing historical data to evaluate system uncertainties and establish boundaries that constrain the optimal charging trajectory of seasonal storage devices. To minimize both total energy consumption over a finite horizon and the value function of seasonal storage at the end of the horizon, the authors formulate a multi-stage stochastic optimization problem.

To tackle the dual challenge of optimizing short-term and long-term decisions, Cuisinier et al. [21] introduced two innovative methods centered around adaptive time-step aggregation. These techniques maintain the continuity of state variables over the long term while ensuring efficient computation times. In the first approach, long-term data and decisions are simplified and aggregated using a simplified long-term model. The second approach involves integrating long-term decisions through cost functions, estimated with representative future data periods and the original detailed model. The approaches are evaluated within the context of a heat production problem, showing promising performance of both approaches and highlighting their potential for integration into rolling horizon approaches.

An approach based on an Affine Adjustable Robust Optimization model is presented by Castelli et al. [22]. This model integrates day-ahead scheduling, unit commitment, and economic dispatch with real-time operational adjustments within a rolling horizon algorithm. Taking into account diverse inputs such as day-ahead forecasts, performance expectations, and target charge levels for seasonal storage, the model optimizes over representative years derived from historical data. This approach addresses the management of energy systems subject to yearly performance constraints and seasonal storage while effectively accounting for short-term forecast uncertainties.

From the presented works, it is evident that finding the best way of incorporating both short- and long-term objectives in smart controllers for the management of seasonal storage is an open issue in the scientific literature, and many strategies have been developed and tested to achieve this goal.

Nevertheless, the presented studies focus on splitting the optimization problem using a short and a long optimization horizon, but none of them analyzes the possibility to also have a multi-space scale to consider a seasonal storage shared among different MES. In this framework, a further step was made in this work, where a novel smart control architecture is proposed, which has a multi-time and multi-space scale, allowing the management of a synthetic methane seasonal storage unit among multiple MES. The novel control architecture allows the real-time control of MES, which is essential for an optimal management, and the consideration in the control strategy also of the yearly dynamics which affect the system and the seasonal storage. This ability is necessary when real-world seasonal storages are implemented, in order to have a meaningful operation and exploit at best their capabilities. The controller was developed in a generalized way, resulting in an approach that can be easily applied to any type of storage.

1.2. Scope of this work

Based on the presented literature review, it is evident that effective management tools play a pivotal role in facilitating the transition toward a fully decarbonized energy sector. In the development of such tools, their versatility, defined by their capacity for easy adaptation to various applications, becomes crucial for their widespread use across diverse scenarios, including energy systems of varying sizes and configurations.

With this in mind, the objective of this study is to introduce an innovative tool designed for the optimal management of electrofuel seasonal storage integrated among multiple MES. Notably, the following novel features are presented:

- A computationally efficient Mixed-Integer Linear Programming (MILP) optimization algorithm, formulated for general MES. This algorithm is easily adaptable to different case studies, efficiently computes the optimal day-ahead energy schedule for the system, and was embedded in an MPC module for the real-time control of MES.
- A stochastic Linear Programming (LP) algorithm, capable of considering multiple MES and a seasonal storage shared among them. It was used for the development of a supervisory MPC module, capable of having a holistic view of the entire problem.
- A novel multi-temporal and multi-spatial control architecture based on MPC, designed to consider both the yearly dynamics associated with the management of seasonal storage and the issue of unit commitment in the short term.

The paper is structured as follows: Section 2 presents the methods employed and the novel control architecture developed; in Section 3 the application is described, namely the case study simulated and the control implementation; Section 4 presents the results obtained from the simulations; and finally in Section 5 the conclusions of the work are discussed.

2. Method

This section introduces an innovative approach for the optimal control of a synthetic methane seasonal storage facility, shared among different energy systems. The presented control architecture leverages the MPC strategy and incorporates two distinct control modules, each operating on different space and time scales.

2.1. Control architecture description

As introduced in Section 1, it is widely acknowledged that renewable fuels produced through PtG systems stand out as one of the most promising solutions to address the growing demand for seasonal storage. However, the intelligent management of an energy system integrated with seasonal storage poses a significant challenge. Indeed, yearly dynamics related to renewable generation and energy demand must be carefully considered. Moreover, when a seasonal storage facility is shared among multiple systems, the coordination of the different systems is not straightforward and requires a comprehensive view of the entire system. In the design and development of intelligent controllers for such systems, it becomes imperative to account for these factors. Consequently, a novel control architecture has been developed to enable the optimal management of a shared methane seasonal storage facility in this specific application. The control action is able to handle real-time energy exchanges while considering both daily and yearly dynamics and the interactions of the different systems with the seasonal storage facility. The schematic representation of the control architecture for a synthetic methane seasonal storage shared among three multi-energy systems is illustrated in Fig. 1.

The developed approach is characterized by a multi-temporal and multi-spatial nature, and uses two distinct control levels: a supervisory long-term MPC that is able to tackle yearly dynamics related to the seasonal storage and a short-term MPC module that is repeated for each MES considered in the application and performs the real-time control of the system, considering additional information coming from the supervisory module. A similar short- and long-term control strategy is proposed in [23]. The two control modules are briefly presented in the following:

- **Supervisory Long-Term Module**: this module is an MPC module with a prediction horizon spanning an entire year and with a daily time-step. This configuration allows the controller to tackle the seasonality in production and demand throughout the year, and to include the management of the seasonal energy storage. Regardless of the number of energy systems considered, the control architecture requires only one supervisory module which includes the entire system. This module computes an optimization every day for the following year, and it is able to account for uncertainty in disturbance forecasts by employing a stochastic LP algorithm.
- **Short-Term Modules**: these modules are replicated for each MES within the application. They consider a prediction horizon of a few days and a short time-step (e.g. one hour). Similarly to the supervisory module, they are designed as MPC controllers and employ a detailed MILP algorithm for optimization. With such a short time horizon, they are not able to optimize seasonal storage management, but instead receive additional information from the supervisory module regarding the optimal daily energy exchange with it. The modules process and transform this information into long-term constraints which are included in the optimization.

The following sections delve into the details regarding the control approach architecture and the specifications of the MPC modules.

2.2. Mathematical model

The two MPC modules contain an optimization algorithm, which is able to optimize the system management over the prediction horizon considered, by making use of simplified models of the systems to control.

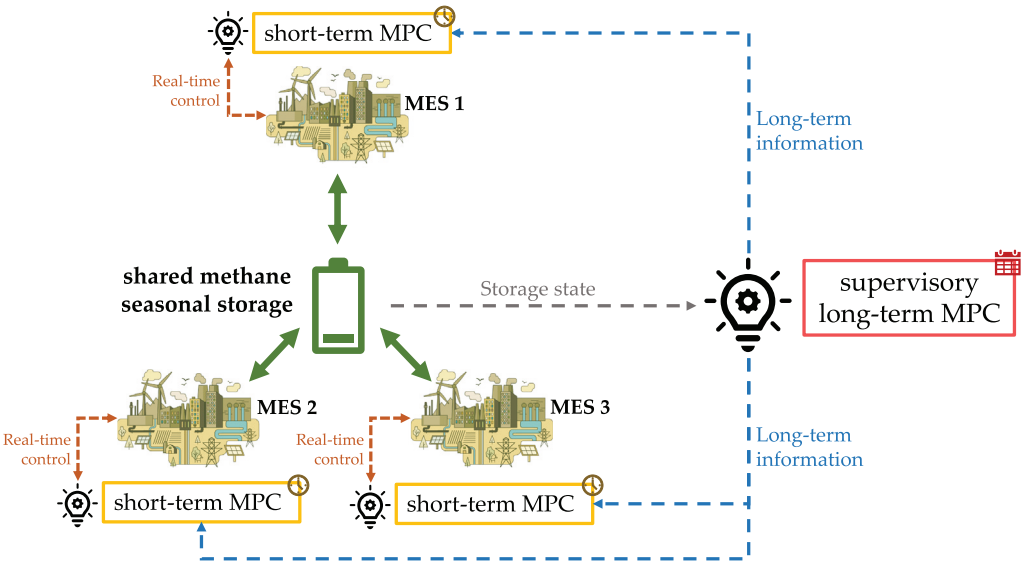

Fig. 1. Multi-temporal and multi-spatial control architecture diagram.

2.2.1. Supervisory module

As previously mentioned, the supervisory module is executed daily and computes the energy exchange requirements between the systems and the seasonal storage throughout the prediction horizon, i.e. one year. The algorithm employed in this module is a stochastic LP algorithm, which was previously developed and validated by the authors as a planning tool in [24]. In this algorithm, the constraints include the energy balances for each energy vector involved, the constitutive equations for the storage facilities and the conversion units. The uncertainties are addressed by generating multiple scenarios every time the algorithm is run, i.e. each day, starting from the future deterministic disturbances. The generation process involves the roulette wheel mechanism to generate the scenarios and a simultaneous backward reduction method to reduce their number, considering both the probability of occurrence of each scenario and their similarity with other scenarios [24–26].

While in the validation phase the algorithm was employed as a planning tool, for the current application it is applied within an MPC approach, and therefore with a rolling horizon approach. In addition, the algorithm has undergone additional tuning to align with the specific requirements of this application, enabling the effective coordination of multiple MES collectively. Basically, each MES is assumed to have its individual energy carriers, and direct energy exchange among different MES is not allowed. Nonetheless, their interconnection is performed through the seasonal storage component, allowing each MES to exchange energy with it. The following equation describes the behavior of the seasonal storage:

$$E_{\text{stor}}(t) = \eta_{\text{sd}} E_{\text{stor}}(t-1) + \sum_{i=1}^{N_z} \left(\eta_{\text{c}} P_{\text{stor}_{\text{in,i}}}(t) - \frac{P_{\text{stor}_{\text{out,i}}}(t)}{\eta_{\text{d}}} \right) \Delta t \,, \tag{1}$$

where N_z is the number of MES in the application, $E_{\text{stor}}(t)$ the amount of energy stored at the current time-step, $E_{\text{stor}}(t-1)$ the amount of energy stored at the previous time-step, η_{sd} the self-discharge efficiency, η_{c} the charge efficiency and η_{d} the discharge efficiency of the seasonal storage. Finally, $P_{\text{stor}_{\text{in,i}}}(t)$ and $P_{\text{stor}_{\text{out,i}}}(t)$ are the power entering and exiting the storage, respectively, at the current time-step for the MES i, and Δt is the time-step length in hours.

Furthermore, a constraint was added to ensure that the quantity of energy stored at the beginning of the prediction horizon equals the energy stored at its end (i.e. one year later). This configuration aligns the algorithm with the concept of seasonal storage, discouraging the system from depleting the storage merely to increase revenues without foreseeing future occurrences. Consequently, the following constraint was incorporated for the seasonal storage, with N_t denoting the total number of time-steps (e.g. 365 for a daily time-step and a one-year prediction horizon).

$$E_{\text{stor}}(0) = E_{\text{stor}}(N_t) \,, \tag{2}$$

where $t = 0$ is the initial time-step and $t = N_t$ the last time-step of the prediction horizon.

The two-stage stochastic programming algorithm was configured with a distinction between first-stage and second-stage variables. The first-stage variables, which are consistent across all scenarios, encompass those associated with the seasonal storage (i.e. the amount of methane entering and exiting the storage facility and the energy stored). Conversely, variables related to other components were classified as second-stage variables, which are scenario specific. This configuration ensures the robust management of the seasonal storage, effectively accounting for the unpredictable nature of future parameters.

2.2.2. Short-term modules

The short-term MPC modules are based on the application developed by the authors for a single MES and tested in [15], where their capabilities are verified. These modules incorporate a detailed MILP algorithm that has proven to be effective in optimizing MES management when tailored to the specific case study, enabling accurate system optimization with reasonable computational complexity. In addition, the global optimality of the solution is guaranteed, and enabled by the usage of available commercial solvers for their solution. Nonetheless, to use such algorithms, the equations describing the physical system must be linearized to derive linear constraints.

The constraints of the algorithm are designed to capture the dynamics of a general MES, and comprise the following components:

- **Conversion Units**: these encompass all plants within the system capable of converting energy from one form to another, such as cogeneration plants, electrolyzers, or heat pumps. The linearization of the input–output relationship is employed to obtain a linear model. To consider efficiency variations with the load, a piecewise linearization method is applied [27,28]. When the output power of the conversion unit only depends on the input power of the unit, a one-dimensional piecewise linear approximation is implemented, which means to perform a piecewise linearization of a function of a single variable. Instead, when the performance

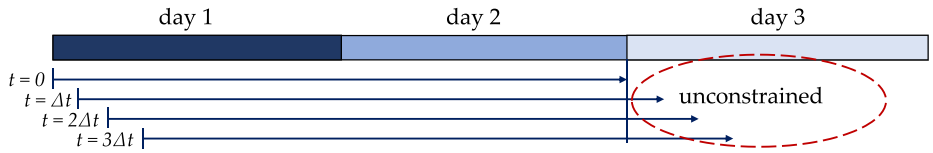

Fig. 2. Diagram of how long-term constraints are given to the short-term modules and how they are used by them.

of a component depends on two external variables, the piecewise linearization has been performed on two dimensions (e.g. the electrical power used to drive the gas compressor depends both on the mass flow rate of the gas and on the pressure ratio, which depends on the storage pressure). The process of approximating a function with a piecewise linear approach in two variables is more complex than in one variable, and various methods can be employed: in this work, the triangle method was utilized [29]. In addition, each plant is capable of working in three operating modes (on, off and standby), characterized by three different input/output relations, with the option to define start-up costs, minimum up-time (UT), minimum down-time (DT), and operating ramps. Additional equations and binary variables are introduced to account for these features.

- **Energy Storage**: this category includes various energy storage methods such as batteries, thermal energy storage systems, and gas storage tanks. The governing equation relates the energy stored at the current time-step to that stored in the previous one, considering charge, discharge, and self-discharge efficiencies.
- **Energy Networks**: depicted as energy sources or energy sinks, the networks allow the systems to purchase or sell energy at specific costs. Examples include electricity grids and natural gas networks.
- **End-users and RES**: represented as energy sources or energy sinks, these entities have specified energy requirements that must be fulfilled, or production rates that serve as external inputs to the algorithm.
- **Energy Nodes**: while not representing physical nodes, energy nodes play a key role in ensuring that the energy balance for each energy vector is maintained during every time-step.

The short-term modules operate with a short time-step and a prediction horizon of two days. Compared to the application described in [15], enhancements were made for the current application, enabling the modules to account for seasonal storage behavior. Indeed, every day at midnight, when the long-term supervisory module is executed, these modules receive information regarding the energy exchange with seasonal storage for the next two days. This information consists of four values: $E_{\text{day1}_{\text{in}}}$, $E_{\text{day1}_{\text{out}}}$, $E_{\text{day2}_{\text{in}}}$, and $E_{\text{day2}_{\text{out}}}$, representing the energy to be injected (in) or withdrawn (out) from storage during the first and second days of the prediction horizon. These values are cumulative over each day, and need further processing for use in the modules, which operate with a shorter time-step. Consequently, they are transformed into constraints for the problem, named *long-term constraints*.

Fig. 2 provides a visual representation of the process, showing the control architecture. Every day at midnight, the long-term module supplies information to the short-term modules for the next two days. The utilization of this information varies depending on the time of day. At the beginning of the day ($t = 0$), when the prediction horizon covers all time-steps for the two days, the value from the long-term module constrains all time-steps for both days. However, as the day progresses, the prediction horizon extends into the third day for the short-term module, where energy exchange information is not yet available. Despite the absence of constraints on time-steps entering the third day, this does not significantly impact the overall functionality of the control action. Indeed, the MPC strategy applies only the first signal to the real system, related to the first time-step of the prediction horizon.

The long-term constraints are given to each MES separately and they are formulated to ensure that the energy injected to or withdrawn from the storage during each day aligns with the values calculated by the long-term module for each of them, allowing a small positive deviation denoted by ϵ. Indeed, to force the achievement of these results, ϵ terms are introduced and minimized in the objective function. This design choice transforms these constraints into *soft constraints*, allowing the variables associated with ϵ to take non-zero values if the system is unable to strictly meet the constraints. This approach prevents the problem from infeasibility issues. For each MES, the formulation of these constraints for the first day of the prediction horizon is as follows, assuming the current time-step to be equal to $\bar{t}$:

$$\sum_{t=\bar{t}}^{N_{\text{d}}-\bar{t}} P_{\text{stor}_{\text{in}}}(t)\Delta t \leq E_{\text{day1}_{\text{in}}} - \sum_{t=0}^{\bar{t}-1} P_{\text{stor}_{\text{in}}}(t)\Delta t + \epsilon_{\text{in}_1}\,, \tag{3}$$

$$\sum_{t=\bar{t}}^{N_{\text{d}}-\bar{t}} P_{\text{stor}_{\text{in}}}(t)\Delta t \geq E_{\text{day1}_{\text{in}}} - \sum_{t=0}^{\bar{t}-1} P_{\text{stor}_{\text{in}}}(t)\Delta t - \epsilon_{\text{in}_1}\,, \tag{4}$$

$$\sum_{t=\bar{t}}^{N_{\text{d}}-\bar{t}} P_{\text{stor}_{\text{out}}}(t)\Delta t \leq E_{\text{day1}_{\text{out}}} - \sum_{t=0}^{\bar{t}-1} P_{\text{stor}_{\text{out}}}(t)\Delta t + \epsilon_{\text{out}_1}\,, \tag{5}$$

$$\sum_{t=\bar{t}}^{N_{\text{d}}-\bar{t}} P_{\text{stor}_{\text{out}}}(t)\Delta t \geq E_{\text{day1}_{\text{out}}} - \sum_{t=0}^{\bar{t}-1} P_{\text{stor}_{\text{out}}}(t)\Delta t - \epsilon_{\text{out}_1}\,, \tag{6}$$

where $P_{\text{stor}_{\text{in}}}(t)$ and $P_{\text{stor}_{\text{out}}}(t)$ denote the power injected and withdrawn from the seasonal storage facility at time step t and N_{d} is the number of time-steps in one day. Finally, ϵ_{in_1} and ϵ_{out_1} are the additional variables added to make these constraints soft. It is important to note that the terms $\sum_{t=0}^{\bar{t}-1} P_{\text{stor}_{\text{in}}}(t)\Delta t$ and $\sum_{t=0}^{\bar{t}-1} P_{\text{stor}_{\text{out}}}(t)\Delta t$ represent the cumulative amount of energy exchanged with the storage during the past time-steps of the day: these values are updated at every time-step using actual data from the real system (or from a model of the system when dealing with its evaluation in a simulation environment).

For the second day of the prediction horizon, the term related to the cumulative amount of energy exchanged is not present, as the current time never extends into the second day. The constraints for the second day are as follows:

$$\sum_{t=N_{\text{d}}-\bar{t}+1}^{2N_{\text{d}}-\bar{t}} P_{\text{stor}_{\text{in}}}(t)\Delta t \leq E_{\text{day2}_{\text{in}}} + \epsilon_{\text{in}_2}\,, \tag{7}$$

$$\sum_{t=N_{\text{d}}-\bar{t}+1}^{2N_{\text{d}}-\bar{t}} P_{\text{stor}_{\text{in}}}(t)\Delta t \geq E_{\text{day2}_{\text{in}}} - \epsilon_{\text{in}_2}\,, \tag{8}$$

$$\sum_{t=N_{\text{d}}-\bar{t}+1}^{2N_{\text{d}}-\bar{t}} P_{\text{stor}_{\text{out}}}(t)\Delta t \leq E_{\text{day2}_{\text{out}}} + \epsilon_{\text{out}_2}\,, \tag{9}$$

$$\sum_{t=N_{\text{d}}-\bar{t}+1}^{2N_{\text{d}}-\bar{t}} P_{\text{stor}_{\text{out}}}(t)\Delta t \geq E_{\text{day2}_{\text{out}}} - \epsilon_{\text{out}_2}\,, \tag{10}$$

where the symbols are consistent with those used for the first day, but they pertain to day 2 of the prediction horizon.

3. Application

The proposed approach was applied to a case study and assessed using a Model-in-the-Loop (MiL) application, i.e. tested on a detailed mathematical model of the system, serving as a digital-twin of the real system. The details of the case study and the implementation are presented in the following sections.

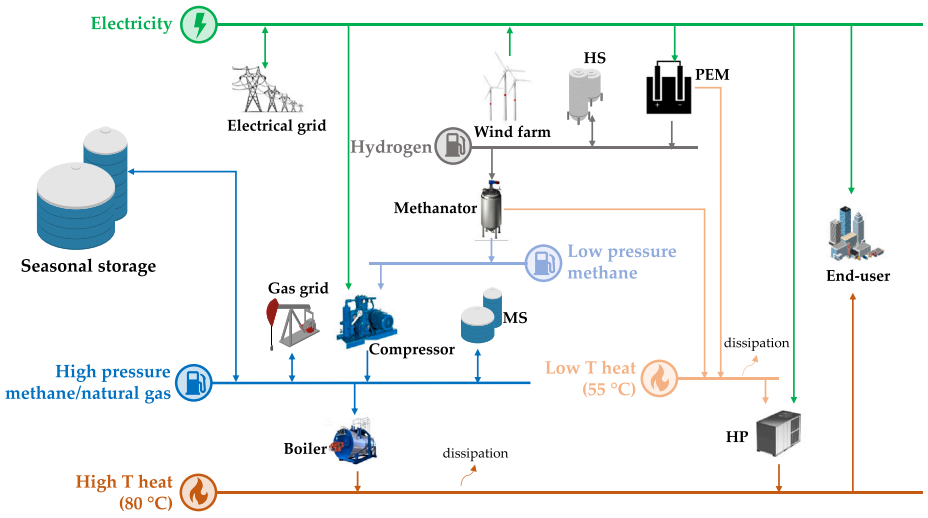

Fig. 3. Diagram of MES 1 and 2. (HS = Hydrogen Storage, MS = Methane Storage, HP = Heat Pump, PEM = Proton Exchange Membrane Electrolyzer).

3.1. Case study description

The case study comprises three MES, all engaged in the generation of synthetic methane through a PtG process. Each system has an electrolyzer for hydrogen production and a methanation reactor for synthetic methane synthesis. The produced gas can be utilized internally within the systems or stored in a shared seasonal storage facility. The overall architecture is depicted in Fig. 1. The three systems exhibit distinct layouts outlined below.

MES 1: a simplified representation of the energy system is illustrated in Fig. 3. It incorporates a PtG plant for synthetic methane production, utilizing renewable electricity generated by a wind farm. The energy system is connected to both the electrical grid and the natural gas network, and it can exchange electricity and gas by buying or selling them. The end-user has both electrical and thermal needs. Electrical requirements are met by using renewable electricity or by purchasing electricity from the power grid, while thermal needs are satisfied using a District Heating Network (DHN), supplied by a gas-fueled boiler and by recovering waste heat from the PtG plant. For recovering the waste heat from the process, a Heat Recovery Circuit (HRC) is employed, which recovers waste heat from the PEM electrolyzer (55 °C), the condenser (80 °C), and the methanation reactor (290 °C). Since the heat recovery is done using a single water circuit, with the three sources in series, the delivered temperature reached by the water is equal to 55 °C. For this reason, an industrial heat pump (HP) connects the HRC with the DHN, which operates at higher temperatures, i.e. between 60 °C and 80 °C, upgrading heat from 55 °C to the 80 °C required by the DHN for end-user heat supply. For clarity of the figure, the condenser is not represented in Fig. 3. The system is also connected to the shared methane seasonal storage facility, allowing energy exchange by injecting or withdrawing gas. The plant characteristics are presented in Table 1.

MES 2: the architecture of MES 2 is identical to that of MES 1 (refer to Fig. 3), with plant sizes and end-user demand scaled by a factor of 1.5. This scaling enables control strategy benefits to be validated for larger energy systems.

MES 3: the architecture of MES 3, which is different from the other two, is depicted in Fig. 4. This system is connected to both the electrical and gas networks, enabling energy exchange by buying or selling it, similarly to the other two systems. However, instead of a wind farm, MES 3 features a photovoltaic plant for renewable energy generation. In addition, unlike the other systems, it does not consider heat recovery from the PtG plant and internal storage for methane is omitted in MES 3. Instead, it incorporates a Thermal Energy Storage (TES) system designed for storing thermal energy in the form of hot water.

By incorporating systems of varying sizes and architectures, the strategy is tested under different conditions, highlighting the general applicability of the developed approach. Detailed specifications for each system are provided in Table 1.

3.2. Implementation

The developed control architecture was tested by applying it in a MiL configuration. A digital-twin of the case study was developed in the MATLAB®/Simulink® environment, utilizing an in-house library of energy system components (for further details, see [15,30]). The models used to build the digital-twin platform are not linear and take into account different system operating modes (i.e. on, off and stand-by).

The MiL application is schematically represented in Fig. 5. Every day, the long-term module (i) receives the State of Charge (SoC) of all the storage units in the system as initialization variables, (ii) performs stochastic optimization over one year, and (iii) communicates to the short-term modules the calculated amount of energy to exchange with the seasonal storage facility each day. The short-term modules are executed every hour, and (i) they receive the SoC of the storage units in the systems as initialization variables (except for the seasonal storage), (ii) use the MILP algorithm for optimization, and (iii) return the optimal set-points for the first time-step to the digital-twin. These set-points encompass the operating mode and the load of the conversion units, the amount of gas to exchange with the gas network, and the amount of gas to exchange with the seasonal storage.

The long-term supervisory module was configured with a prediction horizon of one year and a daily time-step. Every day, 500 scenarios are generated for renewable energy production, as well as the electrical and thermal needs of the end-users. Subsequently, they are reduced to 30 scenarios with the aforementioned simultaneous backward reduction method. The optimization objective is the minimization of total CO_2 emissions, which comprise all emissions associated with the electricity and gas bought from the networks. In this way, the renewable energy utilization is maximized, and the energy security of the systems is increased. The objective function is expressed as the sum of the energy purchased from the networks multiplied by the related emission factors, and is formulated as follows:

$$\min f_{\mathrm{obj_{LT}}}\,, \tag{11}$$

with

$$f_{\mathrm{obj_{LT}}} = \sum_{t=1}^{N_t}\sum_{s=1}^{N_{\mathrm{scen}}} Pr(s)\left(P_{\mathrm{el,bo,s}}(t)e_{\mathrm{CO_{2,el}}} + P_{\mathrm{g,bo,s}}(t)e_{\mathrm{CO_{2,g}}}\right)\Delta t\,, \tag{12}$$

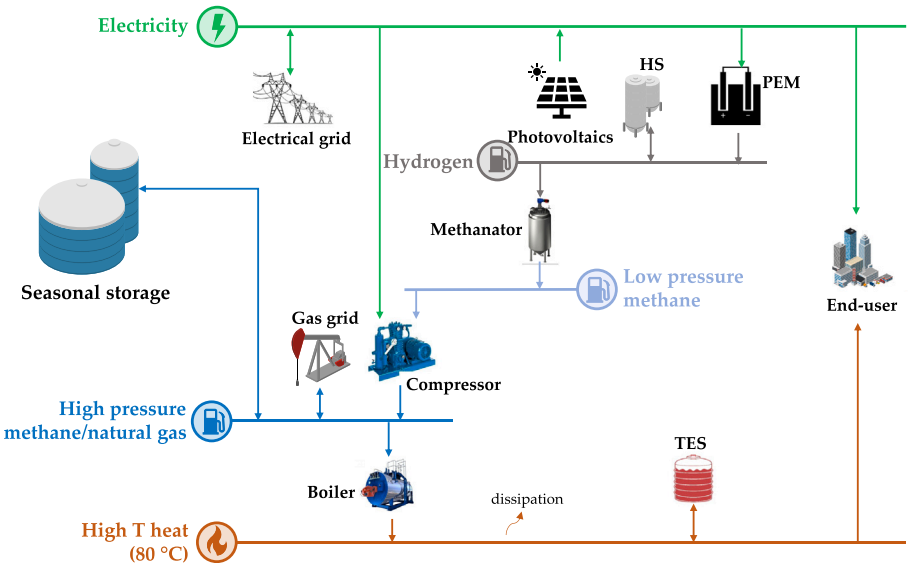

Fig. 4. Diagram of MES 3. (HS = Hydrogen Storage, PEM = Proton Exchange Membrane Electrolyzer, TES = Thermal Energy Storage).

Table 1
Characteristics of the components of the three systems analyzed.

Technology	Parameter	Unit	MES 1	MES 2	MES 3
Wind Farm	Nominal power	(kW)	8000	12 000	–
Photovoltaics	Nominal power	(kW)	–	–	8000
Electrolyzer	Nominal inlet power	(kW)	3750	5625	3750
	Nominal operating temperature	(°C)	55	55	55
	Nominal operating pressure	(bar)	35	35	35
Methanator	Nominal inlet power	(kW)	2479	3718	2479
	Nominal operating temperature	(°C)	290	290	290
	Nominal operating pressure	(bar)	2.5	2.5	2.5
Boiler	Nominal inlet power	(kW)	4000	6000	4000
	Nominal efficiency	(%)	92.4	92.4	92.4
Heat Pump	Nominal inlet power	(kW)	380	570	–
H_2 storage	Volume	(m^3)	100	150	100
	Maximum pressure	(bar)	35	35	35
	Minimum pressure	(bar)	2.5	2.5	2.5
Methane storage	Volume	(m^3)	100	150	–
	Maximum pressure	(bar)	7.5	7.5	–
	Minimum pressure	(bar)	3.5	3.5	–
Thermal energy storage	Maximum capacity	(kWh)	–	–	12 000

where N_{scen} is the number of scenarios, $Pr(s)$ the probability of scenario s, $P_{el,bo,s}(t)$ and $P_{g,bo,s}(t)$ the average amount of electricity and natural gas purchased form the networks, in kW. The emissions related to the electrical grid are calculated using the Italian carbon intensity of electricity generation in 2022, equal to $e_{CO_{2,el}} = 373$ gCO_2/kWh [31], while a coefficient of $e_{CO_{2,g}} = 200.8$ gCO_2/kWh is assumed for the gas network [32].

The short-term modules are configured with a prediction horizon of two days and an hourly time-step. The objective function is formulated to maximize the total operating margin of the systems, involving the maximization of revenues minus costs. Indeed, the objective of the optimization is to minimize the total economic cost of the system. The cost function also includes the minimization of the ϵ variables introduced for softening the long-term constraints. The cost function is expressed by the following equation:

$$\max f_{obj_{ST}}, \tag{13}$$

with

$$f_{obj_{ST}} = \sum_{t=1}^{N_t} \Big(c_{el,so}(t)P_{el,so}(t) + c_{g,so}(t)P_{g,so}(t) - c_{el,bo}(t)P_{el,bo}(t) + - c_{g,bo}(t)P_{g,bo}(t) \Big) \Delta t - \Big(\epsilon_{in_1} + \epsilon_{in_2} + \epsilon_{out_1} + \epsilon_{out_2} \Big), \tag{14}$$

where $P_{el,so}(t)$ and $P_{g,so}(t)$ are the average amount of electricity and gas sold to the networks, respectively, and $c_{el,so}(t)$, $c_{g,so}(t)$ the revenues related to them, while $P_{el,bo}(t)$ and $P_{g,bo}(t)$ are the amount of electricity and gas bought from the networks, with $c_{el,bo}(t)$ and $c_{g,bo}(t)$ being their costs.

To assess the novel control architecture, simulations were conducted for two distinct periods of the year characterized by different weather conditions: five days in May and five days in November. It is important to note that for the sake of computational burden, a detailed nonlinear dynamic Simulink® digital-twin [15] has been used only for MES 1. Instead, MES 2 and MES 3 are assumed to work as predicted by detailed MILP models, executed on an hourly basis to ensure a comprehensive representation of the behavior of the systems, and a noise was introduced to the results, to simulate a real application. This introduces an element of unpredictability, making the model more representative of a real-world application. As a result, only the outcomes related to MES 1 will be presented.

To compute renewable generation over the year, data from PVGIS [33] was utilized for photovoltaic production, and the Wind Atlas website [34] was used for wind power generation, considering as a location for the study a city in Northern Italy. The deterministic forecasts of the disturbances provided to the long-term supervisory module for MES 1 throughout the year are presented in Fig. 6, where the first and

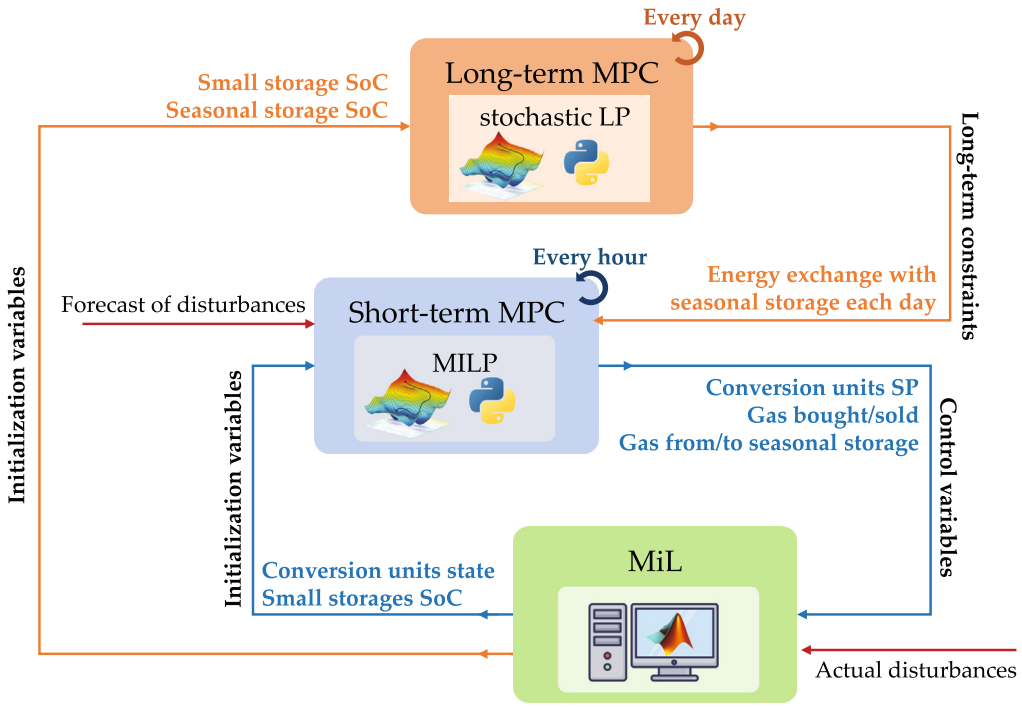

Fig. 5. Diagram of the Model-in-the-Loop application of the control architecture. (SoC = State of Charge, SP = set-point).

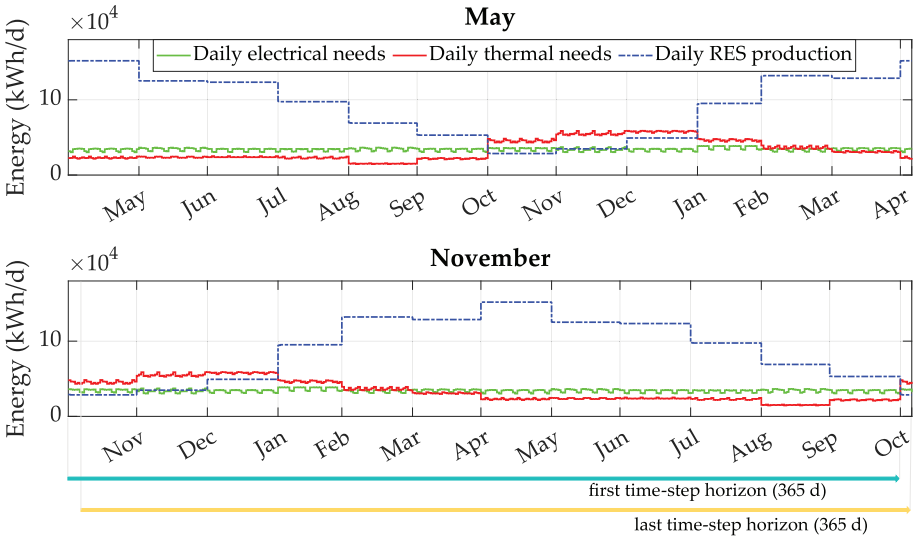

Fig. 6. Forecast of yearly disturbances for MES 1.

last calculation of the long-term MPC for the 5-day simulation are highlighted. This figure illustrates the average daily energy requirements and renewable production, generated by integrating the hourly disturbances over the day. Starting from the deterministic forecast, scenarios utilized in the stochastic approach were generated, using the aforementioned methods [24].

While the long-term module only requires daily average values, a more detailed forecast is employed for the short-term module. The forecasts provided to this module during the two simulated periods are shown in Fig. 7. In this Figure, the prediction horizons of the short-term module for the first and last time-step of the 5-day simulation are also shown. It is worth noting the substantial changes in disturbances between the two seasons. In May, renewable energy consistently exceeds the energy demand, while in November, it is often in deficit, and there are higher thermal requirements.

Finally, in Fig. 8, the costs of purchasing and selling electricity and gas for the two simulated periods are presented.

4. Results

The simulations were executed for the two distinct periods of the year, namely May and November, and the results obtained were analyzed. First, Fig. 9 illustrates the electricity balance, where positive values correspond to generation (RES and purchased electricity), and negative values indicate consumption (user needs, electricity for running the PtG units, including the PEM electrolyzer, the heat pump and the methane compressor, and electricity sold). The figure portrays electricity management within the system during the two simulated periods. In May, the system has a consistent surplus of renewable electricity, therefore there is never the need to purchase electricity

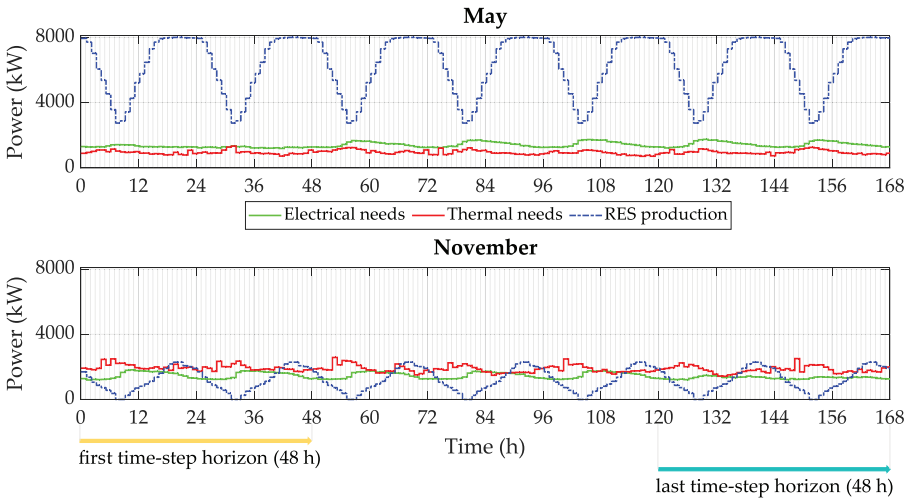

Fig. 7. Forecast of disturbances given to the controller in the two simulated periods for MES 1.

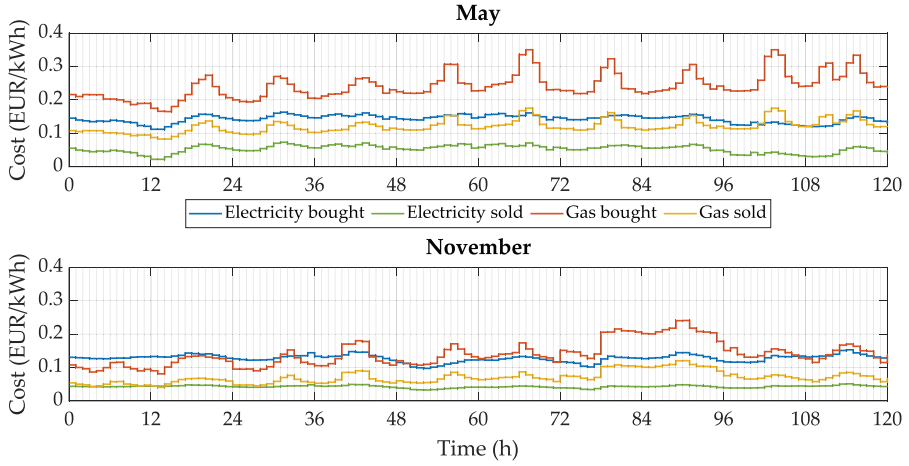

Fig. 8. Energy costs over the two simulated periods.

from the network, and a large amount of electricity is used for running the PtG plant. Moreover, during this period, the system sells the excess generated electricity. In November, instead, there is a deficit in renewable electricity, and the system needs to purchase electricity to meet user needs. Moreover, during this period, there is minimal selling of electricity to the grid. Fig. 10 illustrates the operation of the electrolyzer and the management of the hydrogen storage in the two periods. During May, due to the abundant availability of renewable energy, the electrolyzer operates continuously, and the hydrogen storage is utilized to balance daily energy fluctuations. Conversely, in November, the electrolyzer is activated only during periods of surplus electricity. However, on the first day, the MPC decides to keep it switched off and sell the excess electricity. This decision is driven by additional start-up costs associated with the time required for the system to heat up the electrolyzer stacks. Since the optimization aims to minimize economic costs, it was advantageous for the system to keep the electrolyzer inactive on this day. Indeed, the costs of purchasing and selling electricity and gas vary during the five simulated days, as displayed in Fig. 8. Depending on these costs, the production of gas using the PtG system may be more or less economically convenient. Additionally, as depicted in Fig. 11, during November, the system utilizes the seasonal storage to withdraw methane, compensating for the deficit in renewable generation compared to demands. This allows the system to cover thermal needs during the day without requiring additional hydrogen generation.

In Fig. 11, it can be seen that in November the seasonal storage is solely utilized for withdrawing methane, while in May it is employed exclusively to inject the surplus methane generated. While simulating only five days for each season might not seem to be representative of the entire yearly management of the seasonal storage facility, it is essential to note that the long-term module operates with a yearly prediction horizon, forcing the amount of energy stored at the beginning of the prediction horizon to be equal to the amount of energy stored at the end of the prediction horizon, as expressed in Eq. (2). This implies that the energy exchanges with the storage facility are consistent with what occurs during the remainder of the year. It is not unrealistic that a substantial amount of energy stored in the previous months of the year becomes available in November. Additionally, the long-term module can adapt the management based on the availability of methane in the storage facility, as it receives as input the amount of energy stored in the seasonal storage facility each day.

Fig. 12 illustrates how thermal demand is met during the two seasons. In May, all thermal needs are met using only the generated renewable gas and the heat recovered from the PtG process. This results in a complete decarbonization of the heating sector. In contrast, in November, a portion of the needs (50% of the total demand) is met by purchasing natural gas from the network. Only 2% is fulfilled using the heat pump that recovers waste heat from the PtG process, and 11% is covered by using renewable methane produced by the methanator. Notably, 37% of the needs are addressed by utilizing gas withdrawn

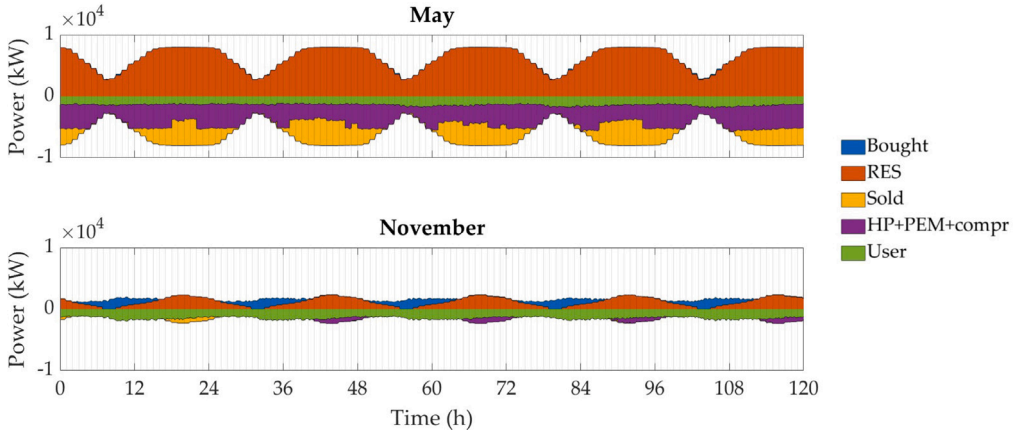

Fig. 9. Electricity balance in the two simulated periods for MES 1. (HP = Heat Pump, PEM = Proton Exchange Membrane Electrolyzer, compr = compressor).

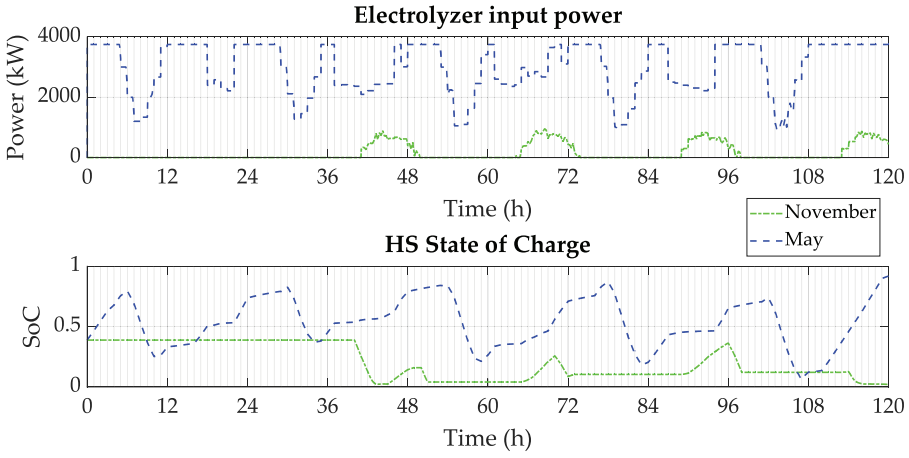

Fig. 10. Electrolyzer and hydrogen storage management during the two simulated periods for MES 1.

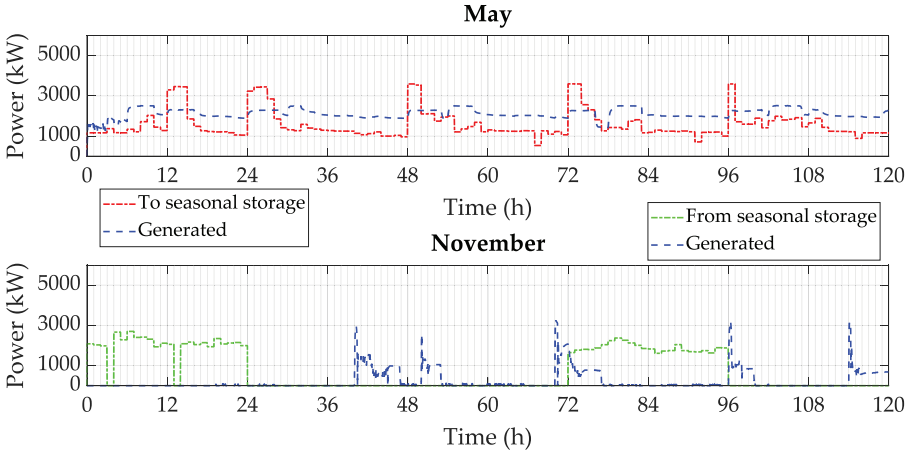

Fig. 11. Amount of methane generated and exchanged with the seasonal storage facility during the two simulated periods for MES 1.

from the seasonal storage facility. Even in this season, half of thermal needs are met using renewable energy, which is made possible by employing the seasonal storage facility. Indeed, renewable generation alone is not sufficient to fulfill the thermal and electrical loads during this season, and the use of seasonal storage allows the utilization of stored energy from periods of higher renewable production.

The amount of gas exchanged with the seasonal storage facility by the three systems during the two simulated periods is displayed in Fig. 13. In May, all three systems utilize the seasonal storage to inject methane, while in November, they withdraw gas to meet the high thermal demand in this season. In both seasons, a daily maximum amount of energy exchanged with the storage facility was set equal to 48 000 kWh, to account for the transmission infrastructure capacity.

A complete fulfillment of the long-term constraints set by the long-term supervisory module was achieved across all three systems, confirming the effective performance of the control architecture. This accomplishment is depicted in Fig. 14 for MES 1, where the cumulative amount of gas exchanged with the seasonal storage (injected in May

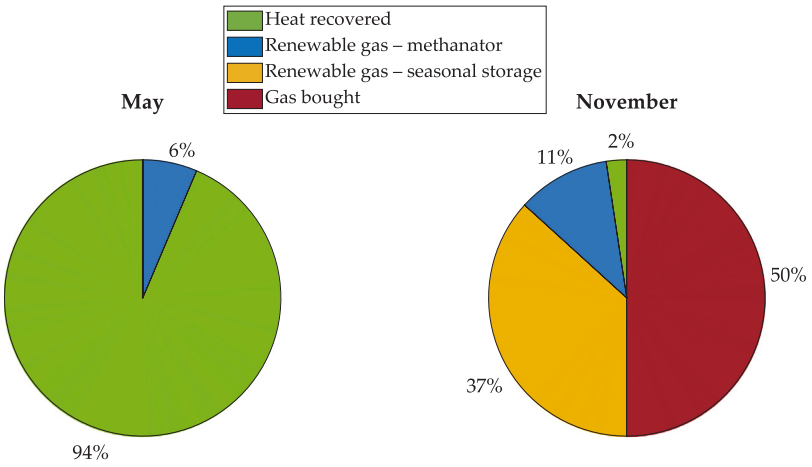

Fig. 12. Pie chart with thermal demand fulfillment in the two simulated periods for MES 1.

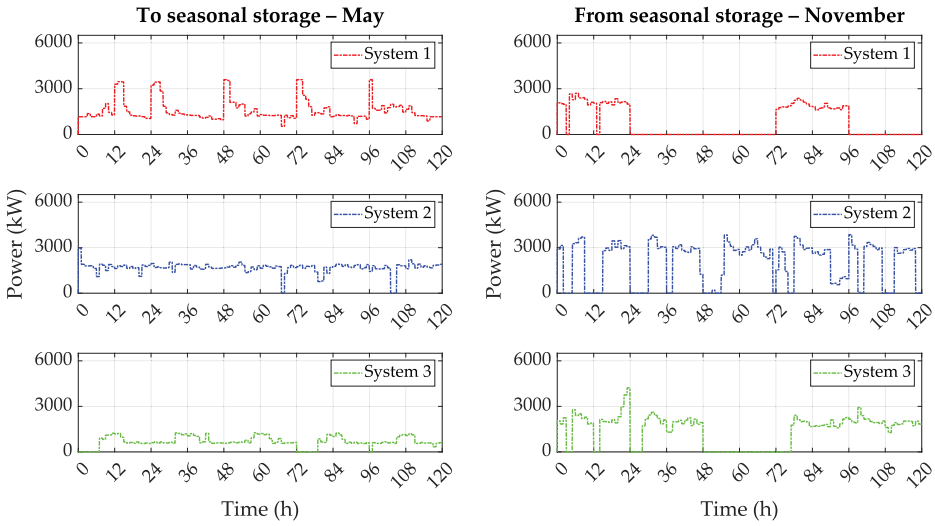

Fig. 13. Power exchanges with the seasonal storage facility during the two simulated periods for MES 1.

and withdrawn in November) is displayed, together with the long-term constraints (in gray) that need to be met each day. This means that all ϵ terms are equal to zero for each simulated day. This is enabled by the fact that the long-term constraints are given to the short-term modules on a daily basis, as depicted in Fig. 2: this means that the short-term controllers have a cumulative constraint to fulfill over each day. Every hour, the short-term modules receive as inputs the actual amount of gas exchanged with the seasonal storage during the past time-steps, which is used to constrain the remaining part of the day using the actual behavior of the system as initial state.

Table 2 presents some cumulative numerical results over the five simulated days. Notably, the operating margin is positive in May, as expected, when a significant amount of renewable electricity is exported. In contrast, it is negative in November, reflecting the need to purchase part of electricity and natural gas to meet internal demands. In addition, the CO_2 emissions, associated with energy imports from the networks, are higher in November. A key outcome is the amount of renewable energy utilized by the system in the two periods, which is not injected into the electricity grid. In May, 71% of RES production is used, while in November nearly all of it is used, reaching 96%. Furthermore, the amount of gas exchanged with the seasonal storage facility is displayed, and the fulfillment of the long-term constraints is highlighted, which are achieved by 100% in both seasons.

While evaluating the control strategy, it is also important to consider the time needed for the algorithms to perform the optimization,

Table 2
Values of relevant indicators obtained in the two simulated periods with the seasonal storage facility for MES 1.

Value	May	November
Operating margin	12 948 EUR	−24 109 EUR
CO_2 emissions	2 286 kg_{CO_2}	49 019 kg_{CO_2}
RES usage	71%	96%
Gas to seasonal storage	189 954 kWh	–
Gas from seasonal storage	–	92 958 kWh
Long-term constraints fulfillment	100%	100%

to analyze the applicability of the method. For the short-term module, the optimization procedure takes a few seconds, while it takes more or less one minute for the long-term optimization. These time intervals are suitable for a real-time application, demonstrating that the method is also a tool for real-world applications.

Finally, by performing the same simulations for MES 1, without the inclusion of the seasonal storage, the results summarized in Table 3 are obtained. In May, the operating margin is higher than in the case with the seasonal storage facility (+ 24 169 EUR), since a larger amount of energy is sold to the networks, instead of being used for storing it, while the CO_2 emissions are slightly lower. Indeed, without the long-term constraints on the seasonal storage, the system can use a larger amount of energy internally. In contrast, the opposite situation happens

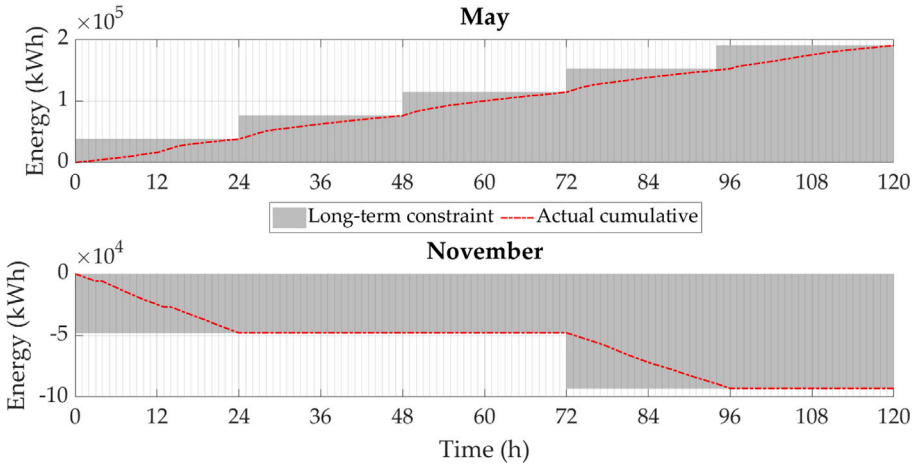

Fig. 14. Fulfillment of long-term constraints by MES 1.

Table 3
Values of relevant indicators obtained with and without the inclusion of the seasonal storage facility for MES 1.

Value	With	Without	Difference
	May		
Operating margin	12 948 EUR	37 116 EUR	+ 24 169 EUR
CO_2 emissions	2 286 kg_{CO_2}	369 kg_{CO_2}	−1 917 kg_{CO_2}
	November		
Operating margin	−24 109 EUR	−38 874 EUR	−14 765 EUR
CO_2 emissions	49 019 kg_{CO_2}	69 051 kg_{CO_2}	+ 20 032 kg_{CO_2}

in November: without the seasonal storage the operating margin is lower (- 14 765 EUR), as the gas needed for fulfilling the heating needs is mainly bought from the network. Indeed, 83% of the thermal needs are satisfied with gas bought from the network, which is 33% more compared to the case with the seasonal storage facility. This also leads to higher CO_2 emissions in this period of the year.

A final consideration regards the assumptions made within the model: as aforementioned, the models used in the controller are linear. For implementing such control strategy in a real-world case study, the linear models should be adapted to the behavior of real components through an identification procedure. Nonetheless, the validation of the control strategy in a simulated environment showed that it works successfully, if the algorithms are properly tailored to the case study considered.

5. Conclusions

Ongoing energy transition is forcing the penetration of non dispatchable renewable energy sources, which require increased energy system flexibility to allow their optimal integration. This flexibility can be enabled, for instance, by including seasonal energy storage units that help mitigate the seasonal imbalances between energy production and demand. Nonetheless, the management of the system obtained is challenging, as a proper control logic for this type of systems is influenced by both daily and seasonal dynamics. To overcome these issues, this work presents a novel hierarchical control architecture, featuring two Model Predictive Control modules operating at multi-time and multi-space scales. This architecture was designed within the context of a case study involving three diverse energy systems, each incorporating Power-to-Gas solutions for synthetic methane generation. It demonstrated notable effectiveness in managing a synthetic methane seasonal storage facility shared among the three systems. The simulations were conducted during distinct periods of the year, specifically in May and November, and provided valuable insights into the performance of the system.

The control strategy exhibited remarkable effectiveness in seasonal storage management. In May, it facilitates the injection of renewable gas into the storage, taking advantage of surplus renewable energy. Additionally, by recovering waste heat from the PtG process and utilizing generated renewable gas, a complete decarbonization of the heating sector is achieved during the simulated period. Conversely, in November, renewable electricity generation alone proves insufficient to meet the energy demand of the system. The control architecture enables strategic purchases of electricity and gas from external networks, optimizing operational costs. Nevertheless, the seasonal storage facility plays a key role during this period, significantly fulfilling thermal demand by using gas withdrawn from storage, with only a small portion met through purchased gas from the network.

The results underscore the effectiveness of the control architecture in optimally utilizing seasonal storage, effectively managing renewable energy generation fluctuations, and ensuring a reliable supply of renewable energy. The short-term modules effectively apply the long-term constraints imposed by the supervisory module, achieving complete fulfillment of such constraints. Moreover, the innovative control strategy, using a holistic view of the entire system, enables strategic decision-making regarding energy sales and purchases, considering market conditions.

In the proposed case study, the long-term supervisory module focuses solely on seasonal storage management as an annual constraint. However, further yearly requirements could be integrated into the long-term module, such as limitations on the maximum quantity of renewable energy exchanged annually with the grid. The addition of further constraints is straightforward in the developed algorithm and could be needed for the incorporation of potential real-world system requirements over the year.

This study highlights the significance of multi-temporal and multi-spatial control strategies in energy systems for enhanced sustainability and efficiency.

In this study, the simulation focused on two distinct periods of the year, in two different seasons. However, to comprehensively assess the effectiveness of the control strategy, future studies will aim to extend the simulation duration to cover longer time periods, potentially encompassing an entire year. Indeed, by investigating longer time periods, the practical applicability of the control strategy in real-world settings could be further evaluated.

Declaration of competing interest

The authors declare that they have no known competing financial interests or personal relationships that could have appeared to influence the work reported in this paper.

Data availability

The data that has been used is confidential.

Acknowledgments

This work was supported by the project "Ecosystem for Sustainable Transition in Emilia-Romagna" (Ecosister), funded under the National Recovery and Resilience Plan (NRRP), Mission 4 Component 2 Investment 1.5 - Call for tender No. 3277 of 30/12/2021 of Italian Ministry of University and Research funded by the European Union – NextGenerationEU (project code ECS00000033, Concession Decree No. 1052 of 23/06/2022 adopted by the Italian Ministry of University and Research, CUP D93C22000460001). This work was co-authored by a researcher with a research contract co-funded by the European Union – PON Ricerca e Innovazione 2014–2020 (according to Italian legislation: art. 24, comma 3, lett. a), della Legge 30 dicembre 2010, n. 240 e s.m.i. e del D.M. 10 agosto 2021 n. 1062).

References

[1] Mancarella P. MES (multi-energy systems): An overview of concepts and evaluation models. Energy 2014;65:1–17.
[2] Sorrenti I, Rasmussen TBH, You S, Wu Q. The role of power-to-X in hybrid renewable energy systems: A comprehensive review. Renew Sustain Energy Rev 2022;165:112380.
[3] Marzi E, Morini M, Gambarotta A. Analysis of the status of research and innovation actions on electrofuels under horizon 2020. Energies 2022;15(2):618.
[4] Guelpa E, Bischi A, Verda V, Chertkov M, Lund H. Towards future infrastructures for sustainable multi-energy systems: A review. Energy 2019;184:2–21.
[5] Barbaresi A, Morini M, Gambarotta A. Review on the status of the research on power-to-gas experimental activities. Energies 2022;15(16):5942.
[6] Bailera M, Lisbona P, Romeo LM, Espatolero S. Power to gas projects review: Lab, pilot and demo plants for storing renewable energy and CO2. Renew Sustain Energy Rev 2017;69:292–312.
[7] Clegg S, Mancarella P. Integrated modeling and assessment of the operational impact of power-to-gas (P2G) on electrical and gas transmission networks. IEEE Trans Sustain Energy 2015;6(4):1234–44.
[8] Liu W, Wen F, Xue Y. Power-to-gas technology in energy systems: Current status and prospects of potential operation strategies. J Mod Power Syst Clean Energy 2017;5(3):439–50.
[9] Alabi TM, Agbajor FD, Yang Z, Lu L, Ogungbile AJ. Strategic potential of multi-energy system towards carbon neutrality: A forward-looking overview. Energy Built Environ 2023;4(6):689–708.
[10] Zong Y, Su W, Wang J, Rodek JK, Jiang C, Christensen MH, et al. Model predictive control for smart buildings to provide the demand side flexibility in the multi-carrier energy context: Current status, pros and cons, feasibility and barriers. Energy procedia 2019;158:3026–31.
[11] Xu Y, Parisio A, Ding Z. Hierarchical model predictive control for energy efficient buildings with multi-energy storage systems. In: 2020 IEEE power & energy society general meeting. IEEE; 2020, p. 1–5.
[12] Zhang D, Han X, Deng C. Review on the research and practice of deep learning and reinforcement learning in smart grids. CSEE J Power Energy Syst 2018;4(3):362–70.
[13] Görges D. Relations between model predictive control and reinforcement learning. IFAC-PapersOnLine 2017;50(1):4920–8.
[14] Nian R, Liu J, Huang B. A review on reinforcement learning: Introduction and applications in industrial process control. Comput Chem Eng 2020;139:106886.
[15] Gambarotta A, Ghionda F, Marzi E, Morini M, Saletti C. Optimal integration of power-to-gas and district heating through waste heat recovery from electrofuel production. In: ECOS2023 - 36th international conference on efficiency, cost, optimization, simulation and environmental impact of energy systems. 2023, http://dx.doi.org/10.52202/069564-0221.
[16] Darivianakis G, Eichler A, Smith RS, Lygeros J. A data-driven stochastic optimization approach to the seasonal storage energy management. IEEE Control Syst Lett 2017;1(2):394–9.
[17] Thaler B, Posch S, Wimmer A, Pirker G. Hybrid model predictive control of renewable microgrids and seasonal hydrogen storage. Int J Hydrogen Energy 2023.
[18] Weber SO, Oei M, Linder M, Böhm M, Leistner P, Sawodny O. Model predictive approaches for cost-efficient building climate control with seasonal energy storage. Energy Build 2022;270:112285.
[19] Petrollese M, Valverde L, Cocco D, Cau G, Guerra J. Real-time integration of optimal generation scheduling with MPC for the energy management of a renewable hydrogen-based microgrid. Appl Energy 2016;166:96–106.
[20] Zhang L, Dai W, Zhao B, Zhang X, Liu M, Wu Q, et al. Multi-time-scale economic scheduling method for electro-hydrogen integrated energy system based on day-ahead long-time-scale and intra-day MPC hierarchical rolling optimization. Front Energy Res 2023;11:1132005.
[21] Cuisinier É, Lemaire P, Penz B, Ruby A, Bourasseau C. New rolling horizon optimization approaches to balance short-term and long-term decisions: An application to energy planning. Energy 2022;245:122773.
[22] Castelli AF, Moretti L, Manzolini G, Martelli E. Robust optimization of seasonal, day-ahead and real time operation of aggregated energy systems. Int J Electr Power Energy Syst 2023;152:109190.
[23] Saletti C, Morini M, Gambarotta A. Smart management of integrated energy systems through co-optimization with long and short horizons. Energy 2022;250:123748.
[24] Marzi E, Morini M, Saletti C, Vouros S, Zaccaria V, Kyprianidis K, et al. Power-to-gas for energy system flexibility under uncertainty in demand, production and price. Energy 2023;129212.
[25] Aghaei J, Niknam T, Azizipanah-Abarghooee R, Arroyo JM. Scenario-based dynamic economic emission dispatch considering load and wind power uncertainties. Int J Electr Power Energy Syst 2013;47:351–67.
[26] Wu L, Shahidehpour M, Li T. Stochastic security-constrained unit commitment. IEEE Trans Power Syst 2007;22(2):800–11.
[27] Bischi A, Taccari L, Martelli E, Amaldi E, Manzolini G, Silva P, et al. A detailed MILP optimization model for combined cooling, heat and power system operation planning. Energy 2014;74:12–26.
[28] Maier L, Schönegge M, Henn S, Hering D, Müller D. Assessing mixed-integer-based heat pump modeling approaches for model predictive control applications in buildings. Appl Energy 2022;326:119894.
[29] D'Ambrosio C, Lodi A, Martello S. Piecewise linear approximation of functions of two variables in MILP models. Oper Res Lett 2010;38(1):39–46.
[30] De Lorenzi A, Gambarotta A, Morini M, Rossi M, Saletti C. Setup and testing of smart controllers for small-scale district heating networks: An integrated framework. Energy 2020;205:118054.
[31] Our world in data – carbon intensity of electricity generation. 2022, https://ourworldindata.org/grapher/carbon-intensity-electricity?tab=table&time=2022..latest&country. [Accessed: 29 Jan 2024].
[32] Specific carbon dioxide emissions of various fuels. 2024, https://www.volker-quaschning.de/datserv/CO2-spez/index_e.php. [Accessed: 29 Jan 2024].
[33] Photovoltaic geographical information system (PVGIS). 2024, https://re.jrc.ec.europa.eu/pvg_tools/en/. [Accessed: 29 Jan 2024].
[34] Global wind Atlas. 2024, https://globalwindatlas.info/en. [Accessed: 29 Jan 2024].